Journal of Catalysis **183,** 344–354 (1999)
Article ID jcat.1999.2419, available online at http://www.idealibrary.com on IDEAL®

Crotonaldehyde Hydrogenation on Pt/TiO_2 and Ni/TiO_2 SMSI Catalysts

Ajit Dandekar[1] and M. Albert Vannice[2]

Department of Chemical Engineering, The Pennsylvania State University, University Park, Pennsylvania 16802

Received October 5, 1998; revised January 4, 1999; accepted January 13, 1999

A kinetic and DRIFTS (diffuse reflectance FTIR) investigation of crotonaldehyde adsorption and hydrogenation was conducted over TiO_2-supported Pt and Ni with the intent of gaining insight into the adsorption modes of molecules with carbonyl groups on these catalysts in the SMSI and non-SMSI states. Significant enhancement in selectivity toward crotyl alcohol was observed with each catalyst after reduction at 773 K. DRIFT spectra under reaction conditions identified crotonaldehyde species strongly adsorbed through the C=C bond and weakly coordinated through both the C=C and the C=O bonds on these catalysts after reduction at 573 K, which gave a peak at 1693 cm^{-1}. After reduction at 773 K, an additional adsorbed species with a strong band at 1660 cm^{-1}, indicating a significant interaction between the carbonyl group and the surface, was observed, which is presumed to be stabilized at interfacial Pt–TiO_x and Ni–TiO_x sites. A decrease in the surface coverage of this species paralleled a drop in selectivity to crotyl alcohol with time on stream. After reduction at 573 K, decarbonylation occurred during the initial few minutes on stream to create adsorbed CO on Pt/TiO_2 in addition to carbon deposition, but these reactions were significantly suppressed after reduction at 773 K, presumably due to a TiO_x overlayer which covers part of the Pt surface and breaks up the ensembles of Pt atoms required for these reactions.

INTRODUCTION

The unique catalytic properties exhibited by TiO_2-supported Group VIII metals after a high temperature reduction (HTR) at 773 K have been clearly demonstrated in a number of reactions during the past two decades (1–4). In particular, overwhelming evidence exists for the promotional role of TiO_2 in enhancing the activities and altering the selectivities in reactions between H_2 and molecules containing carbonyl bonds, such as CO (5–8), acetone (9), crotonaldehyde (10–14), cinnamaldehyde (15), benzaldehyde (16), acetophenone (17), and phenylacetaldehyde (18). A model has been proposed invoking the creation of special sites at the metal–support interface involving partially reduced TiO_x species (or oxygen vacancies) that can coordinate the oxygen atom in the C=O group to account for the selective activation of the carbonyl bonds in these organic molecules (1, 2, 8). The genesis of this strong metal–support interaction (SMSI) behavior has been linked to a high-temperature reduction in the presence of a metal capable of dissociating H_2, thus facilitating the creation of TiO_x species which can migrate and partially "decorate" the metal (1, 2, 4). Although several spectroscopic investigations of TiO_2-supported Group VIII metals exist which have identified features characteristic of these interfacial sites (4), no report of an infrared study could be found in the published literature which identifies the differences in the adsorption modes of molecules with carbonyl groups on these catalysts in the SMSI and the non-SMSI state. The applicability of DRIFTS (diffuse reflectance infrared Fourier transform spectroscopy) to obtain *in situ* spectra during this reaction on supported Cu catalysts has recently been described (19–21). This paper describes a similar kinetic and DRIFTS investigation of crotonaldehyde hydrogenation over TiO_2-supported platinum and nickel catalysts after reduction at either 573 or 773 K.

EXPERIMENTAL

The TiO_2 support used in this study was a 60/120 mesh cut of Degussa P25 (80% anatase, 20% rutile, 50 m^2/g). Nominal 1 wt% Pt or Ni catalysts were prepared by an incipient wetness technique using $H_2PtCl_6 \cdot 6H_2O$ or $Ni(NO_3)_2 \cdot 6H_2O$ (Sigma Chemical Co.) dissolved in distilled deionized water. The TiO_2 was calcined in dry air for 2 h at 773 K prior to impregnation, and the impregnated catalysts were dried at 393 K overnight before storage in a desiccator. Prior to any characterization, the catalyst samples were pretreated *in situ* in flowing He for 1 h at either 573 or 773 K and then reduced in flowing H_2 at the same temperature for 1 h at a typical space velocity of 20,000 h^{-1}. The low-temperature pretreatment at 573 K is 100 K higher than the typical LTR step, while the high-temperature pretreatment (HTR) at 773 K is the same (3, 5–10). Samples with the latter pretreatment will be designated HTR. Total and reversible H_2 uptakes on the pretreated catalyst samples were measured at 300 K in a stainless steel volumetric adsorption system

[1] Current address: Mobil Technology Company, Paulsboro, NJ 08066-0480.

[2] To whom correspondence should be addressed.

0021-9517/99 $30.00

giving a vacuum below 10^{-6} Torr at the sample. The H_2 (99.999% purity, MG Ind.) and He (99.999% purity, MG Ind.) were flowed through molecular sieve traps (Supelco) and Oxytraps (Alltech Assoc.) for additional purification.

The kinetics of vapor-phase crotonaldehyde hydrogenation were determined at atmospheric pressure in the microreactor system described in detail elsewhere (19–21). After loading typically 0.04–0.06 g of catalyst sample in the reactor, it was subjected to reduction at either 573 or 773 K under flowing H_2 and the reactor was then cooled to the desired reaction temperature. Flow rates of H_2 and the diluent He (99.999% purity, MG Ind.) were regulated by mass flow controllers (Tylan, Model FC-260). A constant flow of vapor-phase crotonaldehyde (CH_3–CH=CH–CH=O) was established by bubbling either H_2 or He as the carrier gas through a saturator containing liquid crotonaldehyde (99.9+% purity, Aldrich). Standard conditions for activity runs were 35 Torr crotonaldehyde with the balance H_2 (ca. 700 Torr) and Arrhenius plots were obtained between 323 and 383 K. The data during the Arrhenius runs were obtained after waiting for a period of about 30 min at each set of reaction conditions to allow the system to reach steady-state behavior. In addition, an ascending temperature sequence was followed by a descending temperature sequence to check for deactivation. All kinetic measurements were made at atmospheric pressure and under differential conditions as conversions were routinely maintained below 15%.

Details of the modified DRIFTS reactor system used in the present study and the standard procedures employed to record the spectra have been provided earlier (19–21). After loading the catalyst sample into the DRIFTS cell, it was purged overnight with Ar (99.999% purity, MG Ind.) to remove any moisture in the cell. The sample was then subjected to *in situ* pretreatment at the desired temperature and cooled to 300 K, at which point the first interferogram was recorded. This was used as a background reference in the fast Fourier transform analysis of all subsequent interferograms recorded for that particular catalyst (19–21). In an effort to approximate the reaction conditions under which the kinetic behavior was determined, the sample was then heated to the desired reaction temperature and a flowing mixture of 370 Torr H_2 and 15 Torr crotonaldehyde (balance Ar) was introduced into the reactor chamber. The mixture was obtained by bubbling 50% H_2 in Ar (20 sccm) through crotonaldehyde maintained at 273 K in an ice bath. Although the H_2/crotonaldehyde ratio was about the same as that in the microreactor, the partial pressures were around one-half those in the reactor so that no crotonaldehyde condensation would occur in the DRIFTS system. Spectra were recorded for each catalyst as well as for pure TiO_2 under these reaction conditions at the desired reaction temperature. To obtain spectra of CO adsorbed at 300 K on the Pt/TiO_2 samples, the pretreated catalyst was exposed to a mixture of 10% CO (99.999% purity, MG Ind.) and 90% Ar for 30 min before it was purged with pure Ar for 30 min. Interferograms were collected before and after purging the catalyst.

Temperature-programmed oxidation (TPO) profiles for Pt/TiO_2 samples after use in the crotonaldehyde hydrogenation reaction were obtained in a U-shaped Pyrex microreactor system. The sample was placed between two quartz wool plugs and heated from 300 to 873 K in 30 cm^3/min (STP) of a 10% O_2/90% He mixture at a heating rate of 5 K/min. The product analysis was done with a Perkin-Elmer Sigma 3 gas chromatograph equipped with a Chromosorb 102 column maintained at room temperature to separate O_2 and CO_2 at a sampling interval of 3 min.

RESULTS AND DISCUSSION

Irreversible hydrogen uptakes on Pt/TiO_2 and Ni/TiO_2 after reduction at 573 and 773 K are listed in Table 1 along with the fraction of available surface metal atoms (H/Pt_T and H/Ni_T) and surface-weighted average Pt and Ni crystallite sizes when appropriate. The two former ratios represent

TABLE 1

Crotonaldehyde Hydrogenation over Pt/TiO_2 and Ni/TiO_2 $P_{CROALD} = 35$ Torr, Balance H_2, $T_{RXN} = 333$ K

Catalyst	T_{red} (K)	H_2 uptake[a] (μmol/g)	H/M_T	d_{crys} (nm)	Activity[b] (μmol/s/g cat)	TOF[b,c] (s^{-1})	E_{APP} (kcal/mol)	Selectivity[d]
0.82% Pt/TiO_2	573	17.0	0.81	1.4[e]	3.04	0.089	5.6 ± 0.5	15
0.82% Pt/TiO_2(HTR)	773	0.5	(0.019)	—	4.75	4.7	6.4 ± 0.5	69
1.3% Ni/TiO_2	573	22.0	0.20	5.1[f]	1.51	0.034	2.8 ± 0.3	7
1.3% Ni/TiO_2(HTR)	773	1.5	(0.013)	—	1.64	0.55	3.6 ± 0.5	59

[a] Irreversible uptake at 100 Torr at 300 K.
[b] Measured after 30 min on stream.
[c] Based on irreverible H_2 uptake at 300 K.
[d] Initial selectivity to crotyl alcohol.
[e] Based on $d = 1.13/D$.
[f] Based on $d = 1.01/D$.

valid dispersion values (surface atom/total atom) only after reduction at 573 K. The drop in the H_2 uptake on Pt/TiO_2(HTR) has been routinely observed before (3, 4, 7, 10) and has been shown by TEM not to be due to sintering (22), but rather the decrease is caused by partial coverage of the Pt surface by migrating TiO_x species (4, 10, 23). In the case of Ni, although complete reduction may not be achieved at 573 K (4, 5), suppression of H_2 chemisorption following HTR still occurs and again can be attributed to a blocking of surface Ni sites by a TiO_x overlayer (4, 5, 24).

Table 1 lists the steady-state activities, turnover frequencies (based on the H uptakes), and apparent activation energies during crotonaldehyde hydrogenation on the Pt and Ni catalysts, based on crotonaldehyde disappearance to form crotyl alcohol, butyraldehyde, and *n*-butyl alcohol. The corresponding Arrhenius plots are shown in Fig. 1. No large difference exists between the apparent activation energies after reduction at either 573 or 773 K with either Pt or Ni, although the E_{APP} values after HTR are higher in each case. Also, the activation energy is higher for Pt than for Ni. As reported previously for crotonaldehyde hydrogenation over Pt catalysts, markedly higher TOFs are obtained with the Pt/TiO_2(HTR) catalyst (10), and both the TOF (2.8 s^{-1} at 318 K) and the activation energy (6.4 kcal/mol) agree well with earlier values of 1.5 s^{-1} and 7 kcal/mol, respectively (10). A large enhancement in TOF also occurred with the Ni/TiO_2(HTR) sample. Of equal importance, the activity per gram metal (i.e., per g catalyst) increased after the HTR step for each catalyst. The corresponding activity maintenance profiles for Pt/TiO_2 are shown in Figs. 2A and 2B after reduction at 773 and 573 K, respectively. Similar plots for Ni/TiO_2 are shown in Figs. 3A and 3B. The activity was

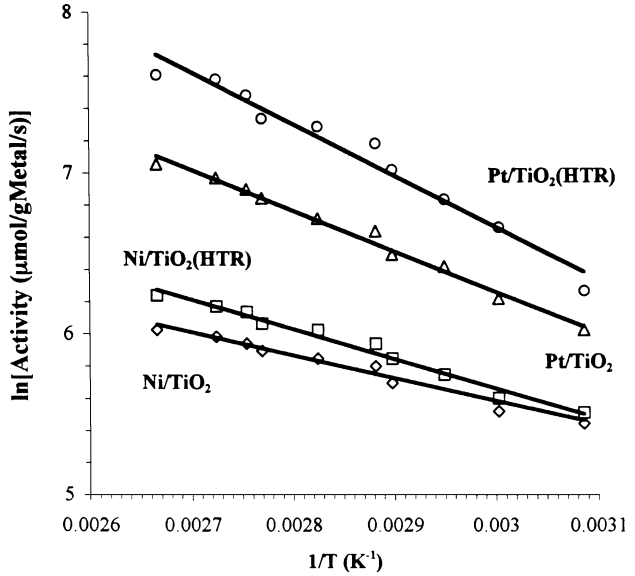

FIG. 1. Arrhenius plots for crotonaldehyde consumption during hydrogenation over Pt/TiO_2 and Ni/TiO_2 reduced at 573 or 773 K (HTR); $P_{CROALD} = 35$ Torr.

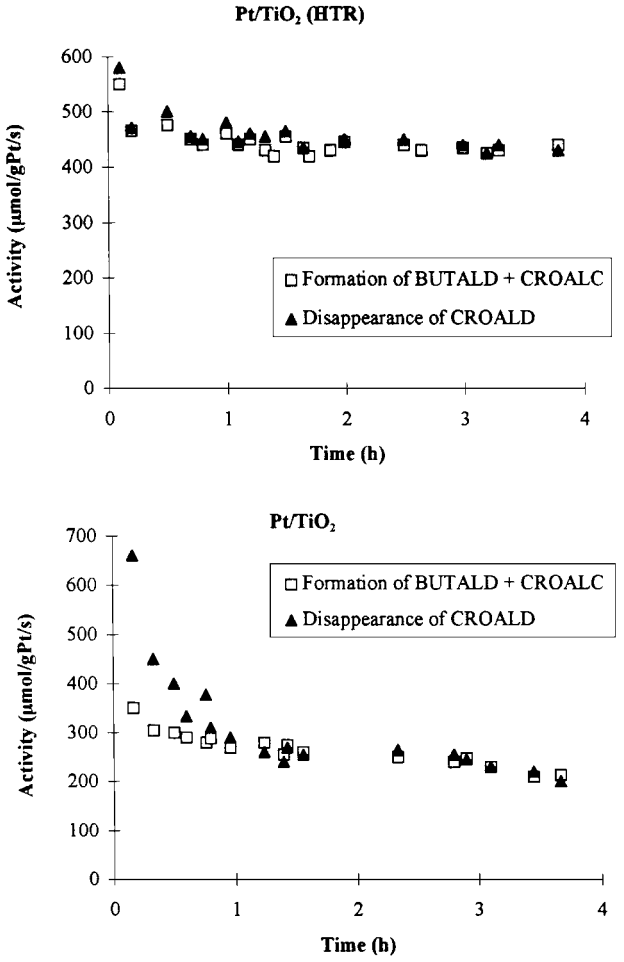

FIG. 2. Activity profiles during crotonaldehyde hydrogenation over Pt/TiO_2 reduced at 573 and 773 K (HTR); $T_{RXN} = 333$ K; $P_{CROALD} = 35$ Torr.

calculated in two ways—either as the rate of appearance of crotyl alcohol and butyraldehyde as products or as the rate of disappearance of crotonaldehyde as a reactant. Whereas no significant difference can be observed between the two methods with Pt/TiO_2(HTR), the rate of crotonaldehyde disappearance is significantly higher than the rate of crotyl alcohol and butyraldehyde appearance during the initial period on stream over Pt/TiO_2 after reduction at 573 K. This suggests that a significant amount of the reactant is consumed elsewhere and suggests the possibility of parallel side reactions like dimerization and decarbonylation (11, 25) or perhaps the formation of coke precursors. In contrast, no significant difference exists between the rates for Ni/TiO_2 after either reduction temperature.

The initial selectivity to crotyl alcohol at 333 K over these catalysts is also listed in Table 1, and a large difference exists between the two Pt/TiO_2 samples or the two Ni/TiO_2 samples. Considerably larger amounts of crotyl alcohol are produced after HTR during the initial hydrogenation period, with the selectivity reaching almost 70% for Pt. As

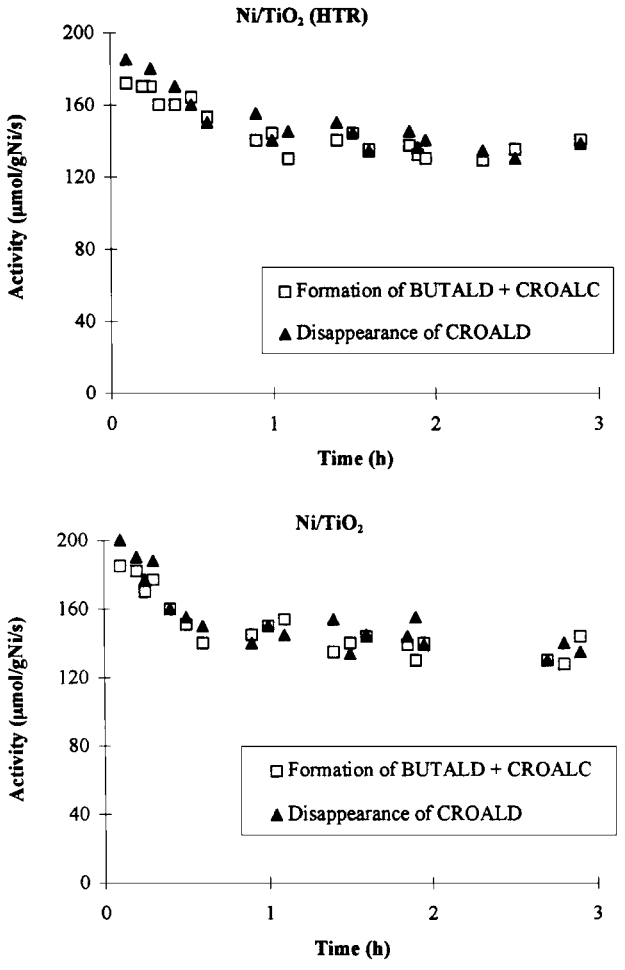

FIG. 3. Activity profiles during crotonaldehyde hydrogenation over Ni/TiO_2 reduced at 573 and 773 K (HTR); $T_{RXN} = 333$ K; $P_{CROALD} = 35$ Torr.

before, this enhancement in carbonyl bond hydrogenation is attributed to special sites created at the metal–TiO_2 interface by TiO_x entities which can migrate and decorate the Pt and Ni particles (1, 2, 10). The coordinatively unsaturated Ti^{+3} (or Ti^{+2}) cations in these suboxide species can interact with the terminal oxygen in crotonaldehyde to activate the C=O bond and enhance its reactivity. The presence of activated hydrogen from the Pt or Ni surface provides for the facile hydrogenation of this group and would not require H spillover over any significant distance (10, 26). There is one report by Lercher and coworkers that an increase in selectivity to crotyl alcohol occurs as Pt crystallites become larger; however, past studies have consistently shown that the HTR step to induce SMSI behavior produces no metal sintering (4, 22). Therefore, the average Pt crystallite size in the two Pt/TiO_2 catalysts should be similar and it is unreasonable to attribute the enhanced selectivity to crotyl alcohol over the Pt/TiO_2 HTR sample to sintering. The corresponding selectivity maintenance profiles as a function of time on stream are shown in Fig. 4. Figures 2 and 3 indicate that deactivation occurs to some extent for all catalysts, but is least noticeable with Pt/TiO_2–HTR and most severe with Pt/TiO_2 reduced at 573 K; nevertheless, once steady state is reached, the activities are relatively constant for significant periods of time. In contrast, the selectivity to crotyl alcohol did not stabilize over any of the catalysts investigated until very low values were reached, which indicates that the Pt–TiO_x and Ni–TiO_x sites favoring crotyl alcohol formation are deactivated faster than those responsible for olefinic C=C bond hydrogenation.

Limited IR studies exist to which the current spectra can be compared. Englisch *et al.* reported spectra taken during this reaction over a Pt/SiO_2 catalyst and identified crotonaldehyde adsorbed on the SiO_2 surface along with CO chemisorbed on Pt (11). They attributed the latter, which was created via a decarbonylation reaction, as being responsible for the observed deactivation. Previously, Waghray and Blackmond had obtained IR spectra during hydrogenation of 3-methyl-2 butenal over Ru/SiO_2 catalysts,

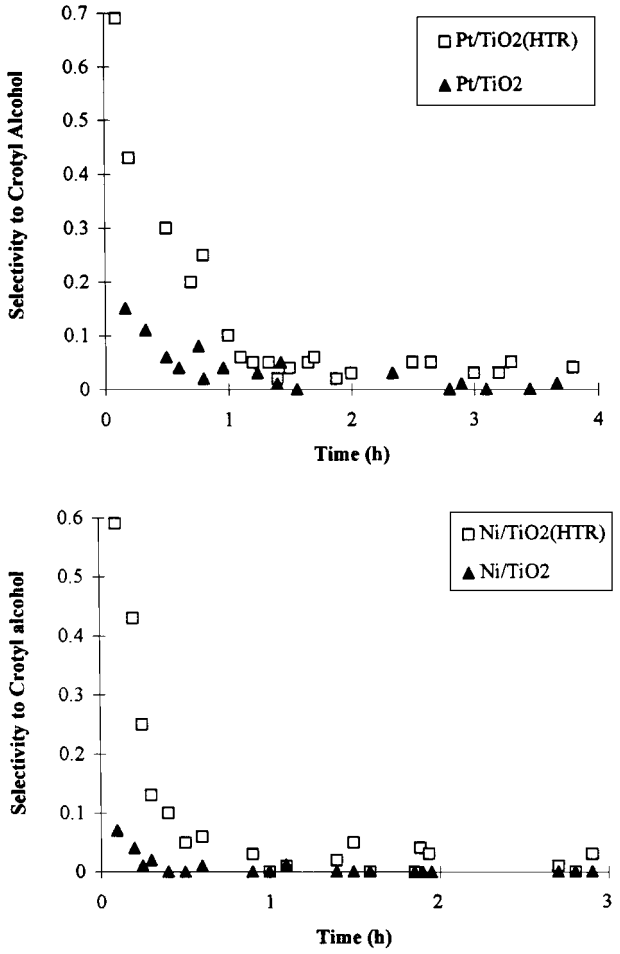

FIG. 4. Selectivity toward crotyl alcohol obtained during crotonaldehyde hydrogenation over Pt/TiO_2 and Ni/TiO_2 reduced at 573 or 773 K (HTR); $T_{RXN} = 333$ K; $P_{CROALD} = 35$ Torr; Conv. = 4–15%.

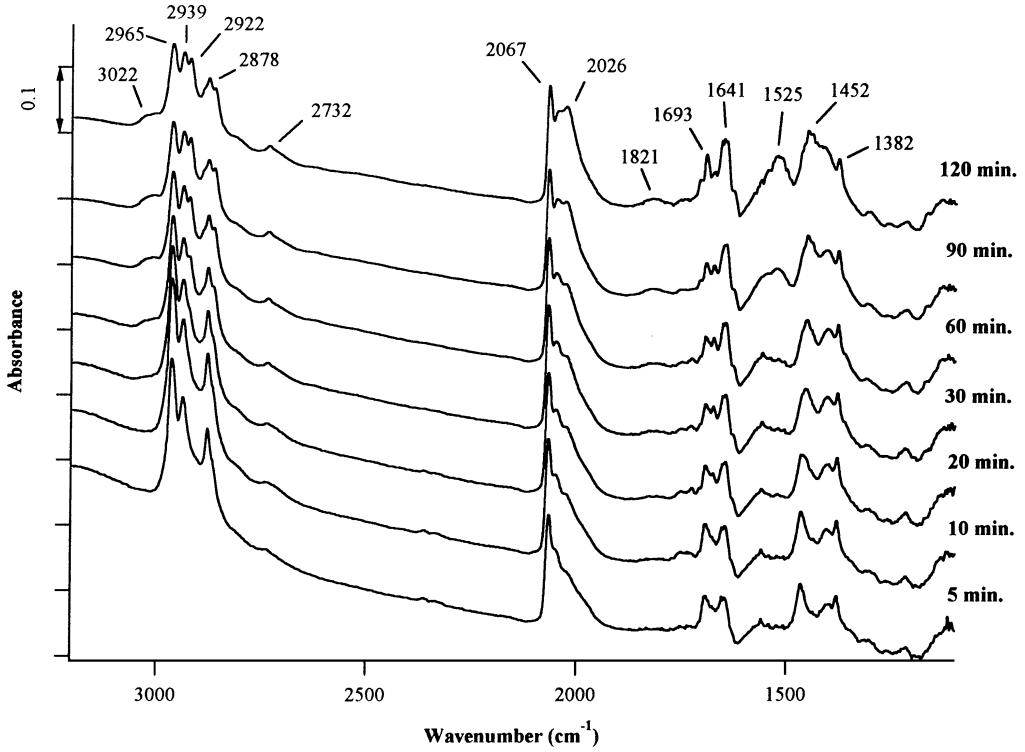

FIG. 5. *In situ* DRIFTS spectra during crotonaldehyde hydrogenation over Pt/TiO_2 reduced at 573 K as a function of time on stream; $T_{RXN} = 333$ K. (Vapor-phase crotonaldehyde spectrum removed.)

and their principal observation was the growth of the peak for chemisorbed CO, which they stated was the cause of activity loss (25). The addition of potassium inhibited this decarbonylation reaction. Neither study reported spectra for TiO_2-supported metals.

In situ DRIFTS spectra acquired during crotonaldehyde hydrogenation at 333 K on Pt/TiO_2 after reduction at 573 K are shown in Fig. 5 as a function of time on stream. The reference spectrum is that of the pretreated catalyst just prior to exposure to the reactant mixture. The vapor-phase spectrum of crotonaldehyde was obtained and subtracted from these spectra. The spectrum obtained after 5 min exhibits bands at 1382, 1465, 1641, 1693, 2067, 2878, 2939, and 2965 cm^{-1}. The 1641 and 1693 cm^{-1} bands can be assigned to the respective C=C and C=O frequencies of crotonaldehyde weakly coordinated on the catalyst surface, as indicated by the small red-shifts from the corresponding vapor-phase frequencies. No bands attributable to a strong coordination through the C=C bond appear to exist. Bands near 1460 and 1375 cm^{-1} are characteristic of the asymmetric and symmetric deformation of CH_3 groups in hydrocarbons perturbed by hydrogen bonding with hydroxyl groups on the TiO_2 surface (27). These bands have been observed before only for crotonaldehyde adsorbed strongly through the C=C bond on supported Cu catalysts (20), but the weak stabilization of crotonaldehyde on Pt via the C=C bond in this case argues against the assignment of 1465 and 1382 cm^{-1} bands to adsorbed crotonaldehyde. The strong bands at 2965, 2939, and 2878 cm^{-1} lie in the frequency region where CH_x stretches in hydrocarbons are usually witnessed (27, 28) and could also correspond to adsorbed crotonaldehyde; however, similar to the peaks at 1465 and 1382 cm^{-1}, the intensity of these peaks is much greater than that expected from the relatively weak peaks at 1693 and 1641 cm^{-1} which correspond to vibrational frequencies characteristic of adsorbed crotonaldehyde. Alternatively, bands around 2970, 2940, and 2880 cm^{-1} have been assigned previously to CH_x stretches in propene adsorbed on transition metals (28), and corresponding wagging deformations have been observed at 1460 and 1380 cm^{-1}. Consequently, it is reasonable to assign the bands at 2965, 2939, 2878, 1465, and 1382 cm^{-1} to olefinic surface species formed due to decarbonylation of crotonaldehyde. Bands around 1693 and 1641 cm^{-1} were also observed in the spectrum of crotonaldehyde adsorbed on pure TiO_2 after reduction at 573 K (21); consequently, a contribution from these bands in the Pt/TiO_2 sample is likely. Similarly, the prominent band at 2067 cm^{-1} with a broad tail lies in the region for CO adsorbed on transition metals and cannot be attributed to adsorbed crotonaldehyde. In conjunction with the activity maintenance profile for this catalyst (Fig. 3) and published literature on Pt/SiO_2 (11) and this band is attributed to

irreversibly adsorbed CO on Pt generated by crotonaldehyde decarbonylation over the catalyst during the initial transient phase.

Several changes occur in the relative peak intensities as the spectra evolve with time on stream. A prominent band develops around 1525 cm^{-1} and the 1452 cm^{-1} band broadens noticeably. The former band can be assigned to crotonaldehyde adsorbed strongly on Pt via the olefinic C=C bond (28). In the CH_x stretching region, a weak peak grows at 2732 cm^{-1} which is characteristic of the aldehydic CH stretch in crotonaldehyde adsorbed weakly via the C=O bond (28), and three new bands emerge at 2922, 2862, and 3022 cm^{-1}. Whereas the former two are characteristic of CH_x stretches in adsorbed crotonaldehyde, the last band has been detected before with supported Cu catalysts (20) and is tentatively attributed to a new C–H bond formed by the addition of one H atom to adsorbed crotonaldehyde. In addition, the broad tail accompanying the 2067 cm^{-1} band grows into a distinct band at 2026 cm^{-1}. The former can be associated with linearly adsorbed CO on Pt, while the latter is due to a dicarbonyl species stabilized on Pt (28). A broad, weak band, characteristic of bridge-bonded CO on Pt, is also detected at 1821 cm^{-1}.

All these bands analyzed together suggest that crotonaldehyde adsorbs both weakly through the C=O and C=C bonds and strongly through the C=C on Pt/TiO_2 after reduction at 573 K, corresponding to the π_{CO}, π_{CC}, and di-σ_{CC} adsorption modes (27, 29), as shown in Fig. 6. Whereas only the π_{CO} and π_{CC} modes are detected on the surface during the initial transient period, the di-σ_{CC} adsorption mode evolves as the system approches steady state. The absence of any detectable surface coverage of crotonaldehyde adsorbed strongly through either of the two unsaturated bonds during the initial transient phase may suggest either the absence of such interactions or the complete consumption of these more strongly coordinated species in the main reaction as well as the parallel decarbonylation reaction, leading to the formation of CO and lower hydrocarbons. If indeed a species adsorbed in the di-σ_{CO} mode does exist during the initial period on stream, it can explain the low but finite initial selectivity toward crotyl alcohol; thus the latter proposal is favored. The appearance of the di-σ_{CC} mode at steady state further supports this proposition. Although one cannot determine exactly which surface sites catalyze each of these individual reactions from the available information, it is possible that as the sites responsible for the decarbonylation reaction as well as crotyl alcohol formation get saturated by irreversibly adsorbed CO and/or hydrocarbon fragments, the overall activity stabilizes, selectivity toward the alcohol drops, and the π_{CO}, π_{CC}, and di-σ_{CC} adsorption modes of crotonaldehyde become visible. Whether these individual η_2(C–C) and η_2(C–O) interactions can occur simultaneously to yield an η_4(C–C–C–O) adsorption geometry, either during the transient phase or

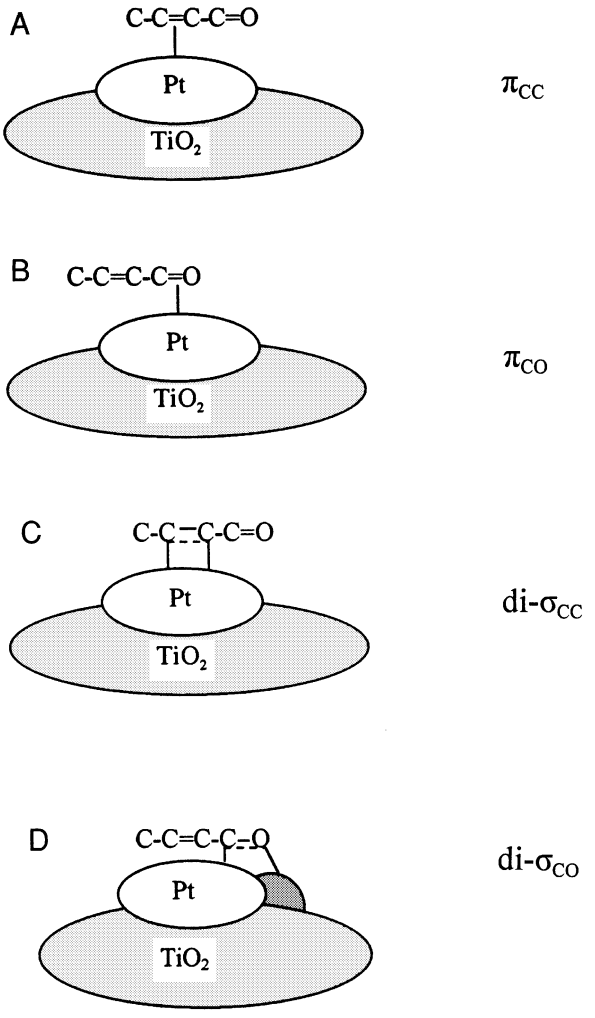

FIG. 6. Different possible adsorption modes of crotonaldehyde over Pt/TiO_2.

at steady state, is difficult to assess from the available data; but, based on mechanistic analyses discussed elsewhere (1, 20, 30), the η_2(C–C) and η_2(C–O) modes seem to be favored on Pt/TiO_2 after reduction at 573 K.

In contrast to Pt/TiO_2, no evidence for decarbonylation or any other side reaction in detected in the spectra of Ni/TiO_2 after reduction at 573 K, as shown in Fig. 7, which is consistent with the kinetic data discussed earlier (Fig. 3). The spectrum obtained after 5 min is very similar to that obtained after 120 min on stream, suggesting minimal changes in the adsorption modes of crotonaldehyde. Figure 7 exhibits absorption bands characteristic of weak π-adsorption of crotonaldehyde through C=O and C=C bonds (1693 and 1636 cm^{-1}), a strong σ-interaction via the C=C bond (1543 cm^{-1}), and the terminal $-CH_3$ deformation modes perturbed due to hydrogen bonding with the TiO_2 surface (1432 and 1376 cm^{-1}). In addition, bands characteristic of CH_x stretches in adsorbed crotonaldehyde are

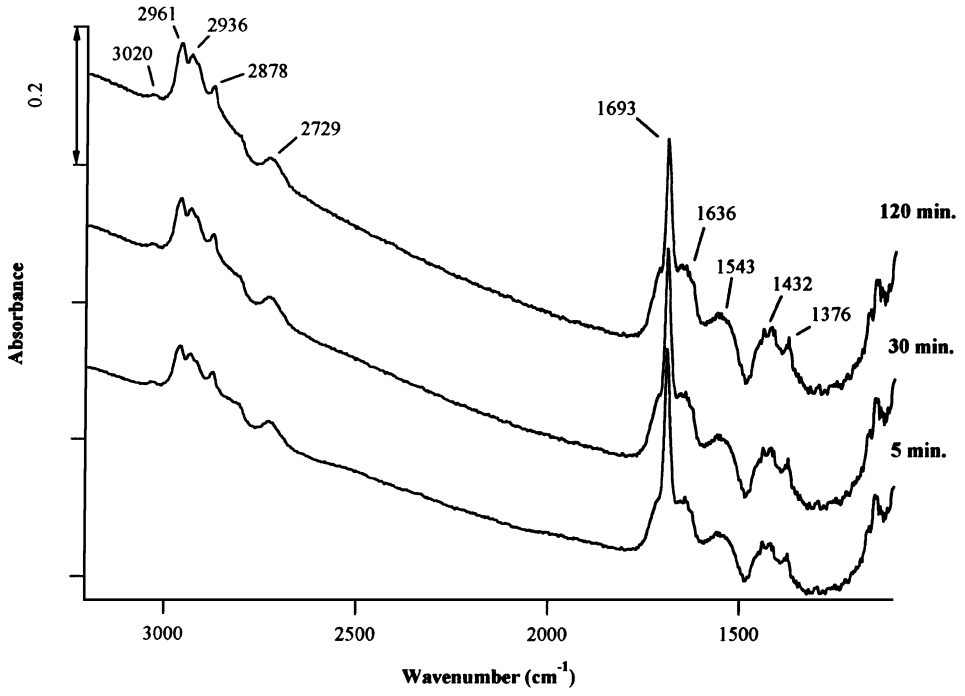

FIG. 7. *In situ* DRIFTS spectra during crotonaldehyde hydrogenation over Ni/TiO_2 reduced at 573 K as a function of time on stream; $T_{RXN} = 333$ K. (Vapor-phase spectrum removed.)

seen at 2961, 2936, 2878, and 2729 cm^{-1} along with a weak peak at 3020 cm^{-1}, which is assigned to a new C–H bond formed after addition of one H atom to crotonaldehyde adsorbed in one of the above forms. Similar to Pt/TiO_2, these π_{CO}, π_{CC}, and di-σ_{CC} interactions can occur independently or simultaneously on Ni/TiO_2 to yield either the η_2 or the η_4 adsorption geometry.

The time-dependent spectra of Pt/TiO_2(HTR) in Fig. 8 and those for Ni/TiO_2(HTR) in Fig. 9 are significantly different from those just discussed. The spectra obtained after 5 min on stream in both cases exhibit one dominant absorption band at 1660 cm^{-1} with shoulders at 1693 and 1630 cm^{-1}. Whereas the latter two bands can be attributed to crotonaldehyde with a weak π-interaction involving the C=O and C=C bonds, respectively (π_{CO} and π_{CC} modes), the shape and position of the 1660 cm^{-1} peak indicate that it can be attributed to a crotonaldehyde species with the C=O bond more strongly coordinated to the catalyst surface, as compared to the weak π-interaction which gives the 1693 cm^{-1} band in most other cases. Spectra for adsorbed butyraldehyde or crotyl alcohol do not provide peaks that correspond to this 1660 cm^{-1} peak (20, 28). Figures 8 and 9 indicate that the surface concentration of this species, which is more strongly bonded through the C=O bond, decreases with time on stream and parallels the drop in selectivity to crotyl alcohol (Fig. 4A and 4B). The fact that this species is detected only after HTR suggests that it corresponds to crotonaldehyde adsorbed on special sites created on the catalyst during the HTR step. Based on these arguments, the 1660 cm^{-1} peak is assigned to crotonaldehyde adsorbed more strongly via the C=O bond in a di-σ mode on interfacial Pt–TiO_x and Ni–TiO_x sites created on these catalysts during HTR. In accordance with the model discussed in detail elsewhere (1, 2, 4, 8–11), the oxygen in the carbonyl groups is envisioned to be coordinated with either Ti^{+3} (or Ti^{+2}) cations at these interfacial sites with the C atom stabilized on a neighboring Pt site, thus leading to a di-σ_{CO} adsorption configuration. The shoulder at 1693 cm^{-1}, assigned to a π_{CO} configuration, and that at 1630 cm^{-1}, associated with a π_{CC} stabilization, indicate that normal weakly adsorbed crotonaldehyde is also present; however, whether these configurations lead to discrete η_2 or overlapping η_4 adsorption geometries is not obvious, but previous analyses of α, β-unsaturated aldehydes adsorbed on catalysts in the SMSI state have favored the η_4(C–C–C–O) adsorption geometry, with the O atom stabilized on the suboxide islands (1, 10, 30). Concurrent with the decrease in the coverage of the di-σ_{CO} species with time on stream is the growth of a strong band at 1548 cm^{-1} and the strengthening of the 1693 cm^{-1} peak, which are characteristic of crotonaldehyde adsorbed in the di-σ_{CC} and π_{CO} configurations, respectively.

As mentioned earlier, the variation in the relative coverages of crotonaldehyde adsorbed in these different modes is synchronous with the shift in the intramolecular product selectivity detected over these catalysts during crotonaldehyde hydrogenation (Fig. 4). This implies that the rate of

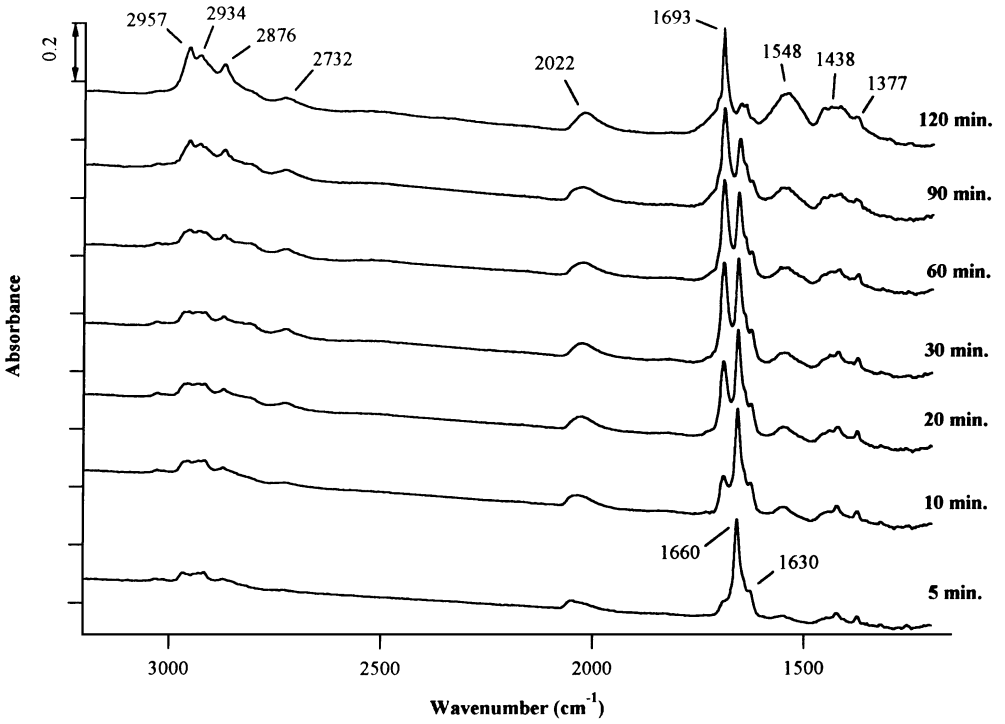

FIG. 8. *In situ* DRIFTS spectra during crotonaldehyde hydrogenation over Pt/TiO_2 reduced at 773 K (HTR) as a function of time on stream; $T_{RXN} = 333$ K. (Vapor-phase spectrum removed.)

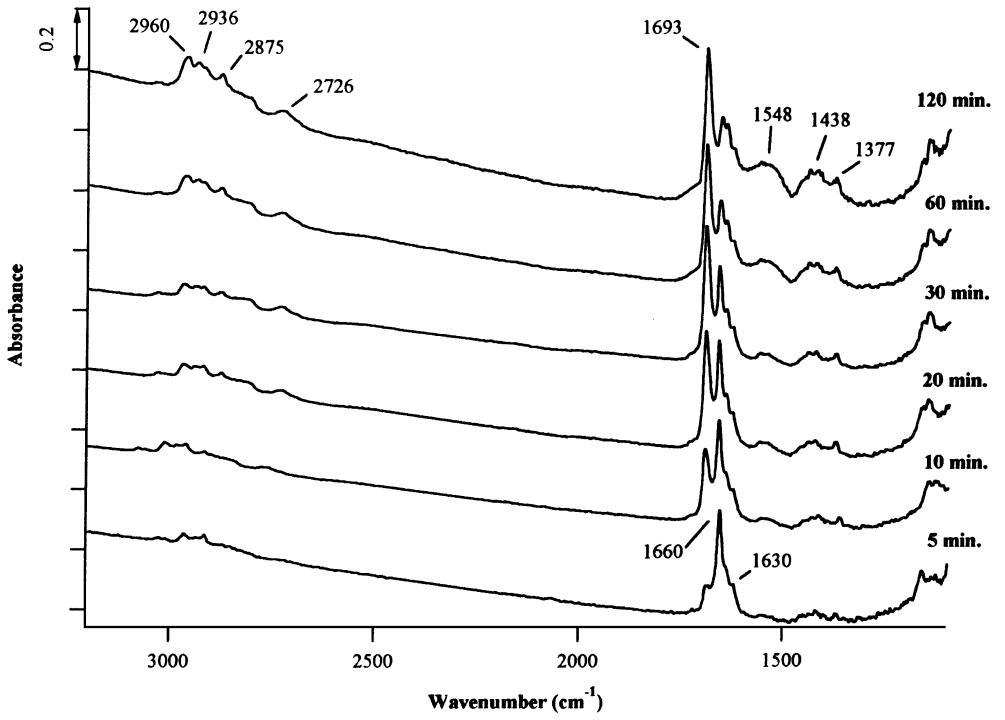

FIG. 9. *In situ* DRIFTS spectra during crotonaldehyde hydrogenation over Ni/TiO_2 reduced at 773 K (HTR) as a function of time on stream; $T_{RXN} = 333$ K. (Vapor-phase spectrum removed.)

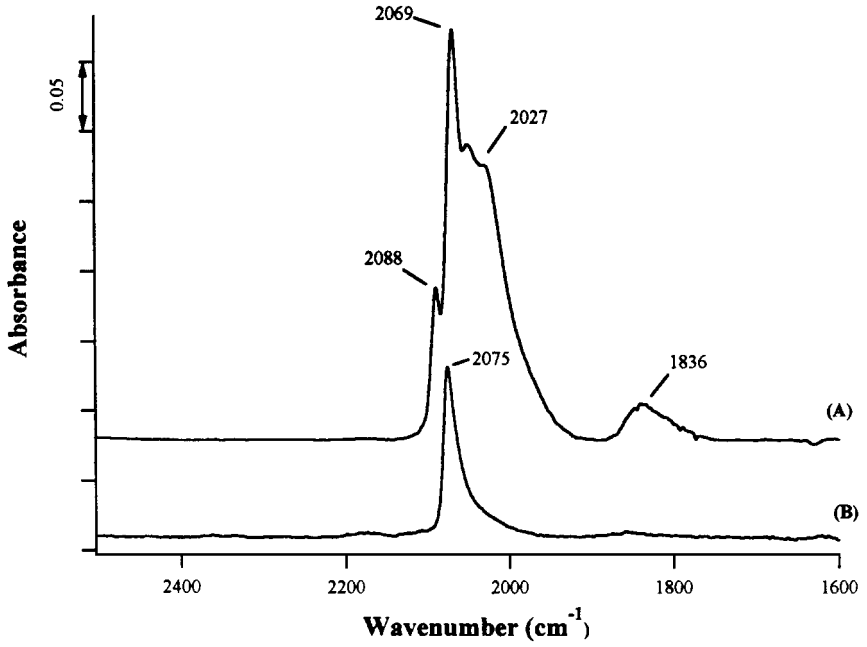

FIG. 10. DRIFTS spectra of CO adsorbed at 173 K on Pt/TiO_2 reduced at: (A) 573 K and (B) 773 K (HTR).

formation of crotyl alcohol is proportional to the surface coverage of crotonaldehyde adsorbed in the di-σ_{CO} configuration at Pt–TiO_x and Ni–TiO_x interfacial sites, leading to the very high initial selectivity toward crotyl alcohol. Evidence to support this hypothesis is provided by plotting the rate of crotyl alcohol formation versus the concentration of this surface intermediate, as represented by the intensity of the peak at 1660 cm^{-1}, and the correlations for Pt/TiO_2 (HTR) and Ni/TiO_2 (HTR) are shown in Fig. 12. An

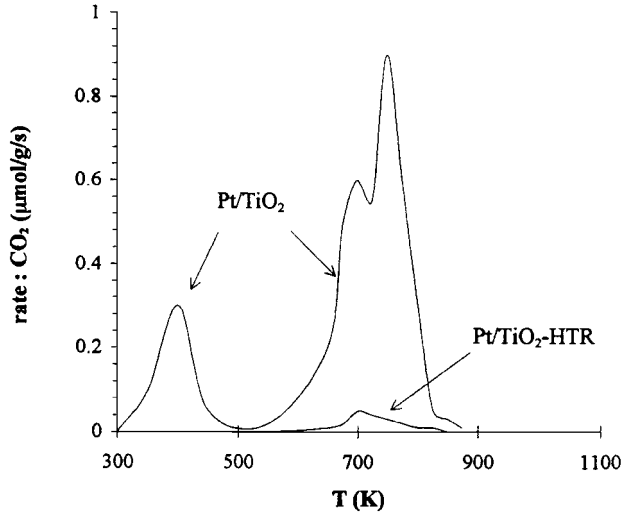

FIG. 11. CO_2 evolution profiles during temperature programmed oxidation (TPO) of Pt/TiO_2 catalysts used for crotonaldehyde hydrogenation; $\beta = 5$ K/min.

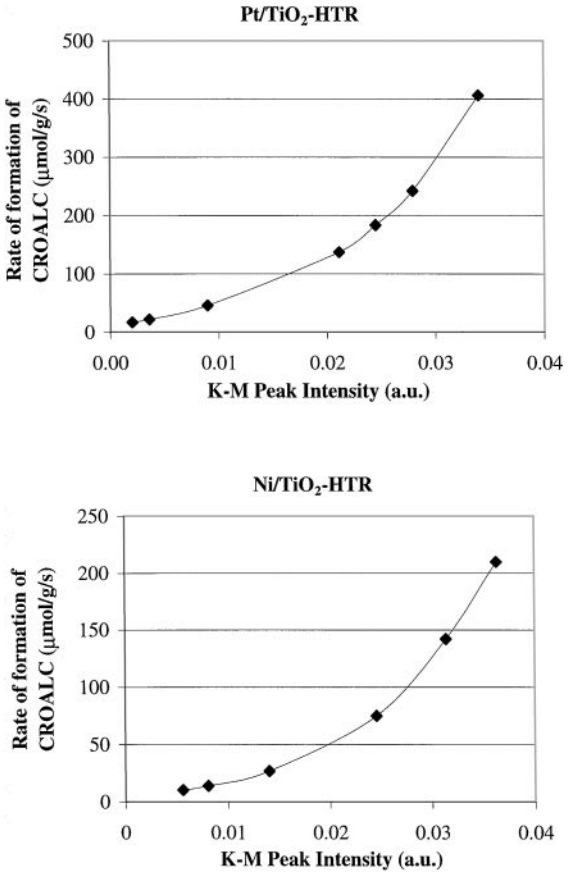

FIG. 12. Correlation of the rate of crotyl alcohol formation with the concentration of adsorbed crotonaldehyde species with a 1660 cm^{-1} band.

obvious dependence exists between crotyl alcohol formation and the surface concentration of this particular intermediate. Although the relationship is not exactly linear, this may well be due to the fact that the rates were obtained from the microreactor data, rather than from the sample in the DRIFTS cell which was operating under one-half the reactant pressures used in the microreactor. The drop in the selectivity to crotyl alcohol, which parallels the decrease in the surface coverage of this species, suggests a reduction in the concentration of these interfacial sites responsible for stabilizing the di-σ_{CO} mode. This could be due to blockage of these sites with irreversibly adsorbed carbonaceous species, reoxidation of these sites, reversal of the SMSI effect due to water possibly formed under reaction conditions, or surface reconstruction leading to formation larger three-dimensional TiO_x islands which decreases the effective metal–support interfacial area. The precise reason is unclear at this point.

An additional feature evident in Fig. 8 is the absence of any significant amount of CO adsorbed on Pt/TiO_2(HTR) after exposure to crotonaldehyde. Only a very weak band can be detected at 2022 cm^{-1} whose intensity slightly increases with time. Spectra of Pt/TiO_2 and Pt/TiO_2(HTR) samples after exposure to 75 Torr CO at 300 K are shown in Fig. 10. With the sample reduced at 573 K, a significant coverage of CO on Pt is indicated by various linear monocarbonyl species with peaks at 2088, 2069, 2050, and 2027 cm^{-1} as well as bridged CO species giving a broad band around 1836 cm^{-1} (28, 31). This latter catalyst was the only one showing extensive deactivation; however, decarbonylation reactions to produce adsorbed CO have been invoked by Waghray and Blackmond (25) and by Lercher and coworkers (11) to explain such losses in activity. A significant decrease in the population of linear carbonyls is observed after HTR, with a single peak at 2075 cm^{-1} remaining and the virtual elimination of the bridged species. This behavior has been observed before and is characteristic of the blocking of Pt sites by migrating TiO_x species (4, 7, 31). In addition to the manifestation of the above effect, the extremely low intensity of Pt–CO bands on the Pt/TiO_2(HTR) sample under reaction conditions suggests a suppression of the decarbonylation reaction after HTR. The TPO profiles of Pt/TiO_2 samples used for crotonaldehyde hydrogenation, shown in Fig. 11, support the above proposal. The CO_2 evolution profile for the catalyst which had been reduced at 573 K prior to exposure to crotonaldehyde exhibits a distinct low temperature peak around 400 K and a high temperature doublet between 700 and 800 K. Whereas the former can be attributed to CO deposited on Pt by decarbonylation of crotonaldehyde, the latter peaks are characteristic of oxidation of carbonaceous deposits formed during hydrogenation reactions (32). These could correspond to the hydrocarbon fragments formed during crotonaldehyde adsorption and decarbonylation over Pt and/or coordinatively unsaturated Ti^{+4} sites, and observed with DRIFTS, or to unreacted crotonaldehyde strongly bound to these surface Lewis acid centers, or to heavier deposits formed due to other side reactions like aldol condensation. In contrast, the HTR catalyst profile exhibits only a very weak band around 700 K, indicating significant suppression of virtually all side reactions leading to adsorbed CO as well as carbon deposition. This is consistent with the activity profile of this catalyst which showed agreement between the rates based either on the formation of detectable products or on crotonaldehyde consumption, and this behavior may be attributed to the formation of the TiO_x suboxide phase reducing the population of surface Ti^{+4} Lewis acid sites as well as an ensemble effect caused by the TiO_x overlayer which destroys Pt sites active for crotonaldehyde decarbonylation.

SUMMARY

A kinetic and DRIFTS study of crotonaldehyde hydrogenation was conducted over TiO_2-supported Pt and Ni with the intent of gaining insight into the adsorption modes of carbonyl group-containing molecules on these catalysts in the SMSI and the non-SMSI states. As reported before, significant enhancement in the selectivity toward crotyl alcohol was observed after reduction at 773 K. DRIFT spectra under reaction conditions identified crotonaldehyde species strongly adsorbed through the C=C bond and weakly coordinated through the C=C and C=O bonds on these catalysts after reduction at 573 K. After HTR, an additional adsorbed species was observed with a C=O peak position at 1660 cm^{-1} that implied a strong interaction between the carbonyl group and the surface, which is attributed to stabilization at interfacial Pt–TiO_x and Ni–TiO_x sites. A decrease in the surface coverage of this species paralleled a drop in selectivity to crotyl alcohol with time on stream. After reduction at 573 K, decarbonylation occurred during the initial few minutes on stream on Pt/TiO_2, but this reaction was significantly suppressed after HTR at 773 K, presumably due an ensemble effect caused by the TiO_x overlayer which removes Pt sites active for crotonaldehyde decarbonylation.

ACKNOWLEDGMENTS

Partial support for this study was provided by the Department of Energy, Basic Energy Sciences Division, via Grant DE-FG02-84ER13276.

REFERENCES

1. Vannice, M. A., *Catal. Today* **12**, 255 (1992).
2. Vannice, M. A., *J. Mol. Catal.* **59**, 165 (1990).
3. Tauster, S. J., Fung, S. C., and Garten, R. L., *J. Am. Chem. Soc.* **100**, 170 (1978).
4. Haller, G. L., and Resasco, D. E., *Adv. Catal.* **36**, 173 (1989).
5. Vannice, M. A., and Garten, R. L., *J. Catal.* **56**, 236 (1979).
6. Vannice, M. A., and Garten, R. L., *J. Catal.* **66**, 242 (1980).

7. Vannice, M. A., and Twu, C. C., *J. Catal.* **82**, 213 (1983).
8. Vannice, M. A., and Sudhakar, C., *J. Phys. Chem.* **88**, 2429 (1984).
9. Sen, B., and Vannice, M. A., *J. Catal.* **113**, 52 (1988).
10. Vannice, M. A., and Sen, B., *J. Catal.* **115**, 65 (1989).
11. Englisch, M., Jentys, A., and Lercher, J. A., *J. Catal.* **166**, 25 (1997).
12. Wismeijer, A. A., Kieboom, A. P. G., and van Bekkum, H., *React. Kinet. Catal. Lett.* **29**, 311 (1985).
13. Makouangou, R. M., Murzin, D. Y., Dauscher, A. E., and Touroude, R. A., *Ind. Eng. Chem. Res.* **33**, 1881 (1994).
14. Raab, C. G., and Lercher, J. A., *Catal. Lett.* **18**, 99 (1993).
15. da Silva, A. B., Jordao, E., Mendes, M. J., and Fouilloux, P., *Appl. Catal. A* **148**, 253 (1997).
16. Vannice, M. A., and Poondi, D., *J. Catal.* **169**, 166 (1997).
17. Lin, S. D., Sanders, D. K., and Vannice, M. A., *Appl. Catal. A* **113**, 59 (1994).
18. Poondi, D., and Vannice, M. A., *J. Mol. Catal. A* **124**, 79 (1997).
19. Rao, R., Dandekar, A., Baker, R. T. K., and Vannice, M. A., *J. Catal.* **171**, 406 (1997).
20. Dandekar, A., Baker, R. T. K., and Vannice, M. A., *J. Catal.*, in press.
21. Dandekar, A., Ph.D. dissertation, The Pennsylvania State University, 1998.
22. Baker, R. T. K., Prestridge, E. B., and Garten, R. L., *J. Catal.* **56**, 390 (1979).
23. Tauster, S. J., *Acc. Chem. Res.* **20**, 389 (1987).
24. Bradford, M. C. J., and Vannice, M. A., *Appl. Catal. A* **142**, 73 (1996).
25. Waghray, A., and Blackmond, D., *J. Phys. Chem.* **97**, 6002 (1993).
26. Neikam, W. C., and Vannice, M. A., *J. Catal.* **27**, 207 (1972).
27. Colthup, N. B., Daly, L. H., and Wiberley, S. E., "Introduction to Infrared and Raman Spectroscopy," 3rd ed. Academic Press, San Diego, CA, 1990.
28. Davydov, A. A., "Infrared Spectroscopy of Adsorbed Species on the Surface of Transition Metal Oxides." Wiley, London, 1990.
29. Delbecq, F., and Sautet, P., *J. Catal.* **152**, 217 (1995).
30. Yoshitake, H., and Iwasawa, Y., *J. Catal.* **125**, 227 (1990).
31. Vannice, M. A., and Twu, C. C., *J. Catal.* **79**, 70 (1983).
32. Querini, C. A., and Fung, S. C., *App. Catal. A* **117**, 53 (1994).